Strong Quantum Dot Photoluminescence Enhancement in Silver Nano-Island Films

Hagen Langhuth, Simon Frédérick, Michael Kaniber, and Jonathan J. Finley
Walter Schottky Institut, Technische Universität München,
Am Coulombwall 3, 85748 Garching bei München, Germany

Ulrich Rührmair
Institut für Informatik, Technische Universität München,
Boltzmannstr. 3, 85748, Garching bei München, Germany
(Dated: June 1, 2010)

We present the fabrication and optical investigation of highly random self-assembled, nano-scale films, probing their influence on the luminescence properties of near surface CdSe/ZnS colloidal quantum dots. When compared to quantum dots distributed on unstructured quartz substrates, the average luminescence intensity is found to be enhanced by a factor of 160×. The silver nanoparticles are prepared using slow thermal evaporation on quartz substrates and post-deposition annealing to produce a randomly-arranged layer of smooth nano-islands. Clear polarization dependent hot spots are observed. Such hot spots deliver a maximal enhancement of the emission intensity of 240× and have a spatial density of $(0.050\pm0.002)\,\mu\mathrm{m}^{-2}$. These results indicate that such silver nanoparticle may be promising candidates for many applications in surface sensing.

Recent advances in plasmonics have renewed interest in the study of the optical properties of thin metallic films. A non-uniform metallic film, patterned on the nano-scale either by advanced electron-beam lithography techniques[1–4] or formed via self-assembly[5–10], can dramatically modify the optical properties of a material in its vicinity. For example, such metallic nanostructures can enhance the absorption strength of proximal or embedded optical materials to realize high efficiency solar cells[1, 2, 6, 9]. The concentrated electric field produced by hot spots in such nanoscale metallic structure s can also lead to large modifications of the spontaneous emission properties[4–6, 11] and, even, suppress fluorescence intermittency[12, 13] and reduce device fatigue[11, 13].

In this letter, we use a simple technique to produce silver nano-island films utilising a combination of slow metallic evaporation and rapid thermal annealing. Our approach produces smooth half-spheroid silver nano-islands. These nano-islands are in strong contrast with chemistry-based techniques that typically produce arrays of spheres[7, 8, 14]. It has recently been shown that half-spheroid metallic nanoparticles scatter the incident light more efficiently into surface plasmon polariton modes, thus coupling more efficiently to the adjacent material; colloidal CdSe/ZnS quantum dots (QDs) in our case[15]. At a controlled separation of 10 nm between the QD layer and the silver film, very large enhancements of the luminescence intensities are observed: an average factor of 160× with intense hot spots yielding factors as high as 240×.

The silver nano-island films used in this work were prepared by slow thermal evaporation of a nominally 10 nm-thick silver layer onto a quartz substrate at 10^{-6} mbar pressure. After deposition, the samples were rapid-thermal-annealed at 250 ^{o}C in forming gas atmosphere for 10 minutes producing rounder, more distinct nano-islands. Figure 1**(a)** shows a typical atomic force microscopy (AFM) image of the obtained surface. The nano-islands formed by this technique are smooth (surface roughness below 0.5 nm) half-spheroids as shown in the surface profile in Fig.1**(b)**. They have a broad Gaussian distribution of diameters and heights, with an average diameter of 50 nm. The full-width at half maximum (FWHM) of this distribution is 40 nm whereas the height is centered at 37 nm with a FWHM of 20 nm. The islands have an areal density of 230±10 nano-islands per $\mu\mathrm{m}^2$. From these values we can derive an average inter-

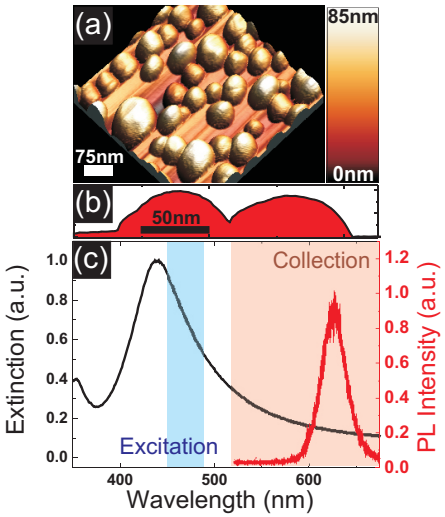

FIG. 1: (a) Atomic force microscopy image of typical silver nano-island film used in this work. (b) Surface profile of two adjacent islands. (c) Typical silver nano-island film extinction spectra (black line) and CdSe/ZnS typical photoluminescence spectra (red line). The shaded blue and red areas highlight the spectral dependance of the excitation and collection filters respectively.

island distance of (16.0±0.7) nm. However, the random assembly process produces a broad distribution in terms of inter-island separation ranging from adjacent islands to distances as large as 100 nm. A 10 nm-thick layer of SiO_2 is then sputtered on top of the as grown samples to serve as a spacer between the silver and the QDs. This allows the QDs to be brought into the near field of the plasmonic resonances whilst preventing luminescence quenching due to charge transfer between the QDs and the silver nanoparticle surface[4, 5]. The extinction spectra of the sample, measured using a Xenon lamp in a Varian Cary 50 microscope system, is presented as the black curve in Fig.1**(c)**. The broad peak from 400-500 nm with a peak wavelength at 440 nm is the ensemble-averaged plasmon resonance of the silver nanoparticles. This wavelength is fully consistent with expectations, given the ∼50 nm lateral size of the silver nanoparticles[9, 13].

The colloidal QDs used in this study have CdSe core with a ZnS shell (CdSe/ZnS). They were dispersed on the silver nano-island film by dilution in Toluene to a concentration of 12 nM and spinning them at 4000 rpm for 40s. The red curve in Fig.1**(c)** shows a typical QD ensemble photoluminescence spectra recorded by exciting with a 405 nm laser with a power density of 70 W/cm^2. It shows a strong peak centered at 625 nm. We notre that the plasmon resonance at 440 nm overlaps strongly with the absorption spectrum of the CdSe/ZnS QDs. We used an Axiovert 200M MAT fluorescence microscope from Zeiss with an ORCA ER Hamamatsu camera to image the resulting fluorescence from our sample. Filters inserted in the microscope select the excitation wavelength range from a mercury vapor lamp to be 450 nm to 490 nm as illustrated by the blue shaded area in Fig.1**(c)**. Hence, the excitation light is absorbed not only by the quantum dots but also excites plasmons in the silver nano-island film. The red shaded area in Fig.1**(c)** shows the wavelength range that is detected by the silicon CCD detector (>515 nm), as selected by a long-pass filter. Fig.2**(a)** shows a typical image of an area of the sample containing both QDs on bare quartz (left panel) and on the silver nano-island film (right panel). The QDs lying on the silver nano-island film emit more strongly than those on the bare quartz. This is due to the combined effect of the increased absorption by the silver nano-island film as well as the increased QDs photoluminescence due to coupling of the QDs to plasmonic radiative modes where the electric field is enhanced. The excitation and acquisition parameters need to be adjusted to properly measure the luminescence of the QDs on both substrates and of the silver substrate itself. Fig.2**(b)** shows the measured QD photoluminescence intensity on quartz with an excitation intensity I_{exc} = 16 W/cm^2 and integration time t_{int} = 936 ms. The silver film luminescence is shown in Fig.2**(c)** (I_{exc}=4.4 W/cm^2 and t_{int}=819 ms). We attribute this luminescence to photoactivated emission in nanoscale silver oxide[16]. In Fig.2**(d)**, we use

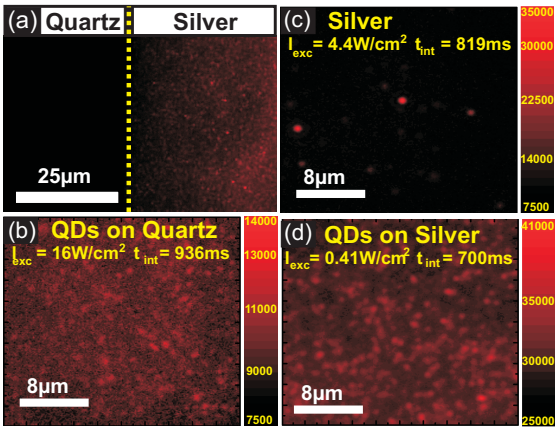

FIG. 2: (a) Photoluminescence of QDs lying on bare quartz (left) and a silver nano-islands film (right) area. Photoluminescence of (b) QDs lying on bare quartz, (c) the silver nano-island film, and (d) QDs lying on silver nano-islands film.

I_{exc} = 0.41 W/cm^2 and t_{int} = 700 ms to image the luminescence of QDs on a silver nano-island film. In this case, most of the energy absorbed by the silver nano-islands will be extracted from the sample by photon emission via QDs. Those images were analyzed by taking the number of counts for each pixel and dividing it by the excitation intensity and the integration time for the maps in **(b)**, **(c)**, **(d)**. The average normalized pixel intensities are measured to be 650, 2 800, and 105 000 counts/(J/cm^2) for the QDs on the quartz substrate, the silver nano-islands without QDs and the silver nano-islands and QDs structures, respectively. The substraction of the silver luminescence from the intensity of the QDs on silver nano-islands film emission shows a 160-fold enhancement of the QD luminescence intensity with respect to their luminescence on bare quartz. This value is the average enhancement, each pixel containing more than 100 QDs.

The granular nature of the QD luminescence on the quartz substrate is attributed to the formation of QD aggregates. Whilst aggregates also form when the QDs are spun onto a silver substrate, a study of the polarisation dependance of those reveals the presence of hot spots. Figure 3**(a)** shows a false color image of the QD photoluminescence on a silver nano-island film. This image was recorded with I_{exc} = 0.41 W/cm^2, t_{int} = 700 ms and without polarization selectivity in the detection channel. The insertion of a linear polariser into the excitation beam path confirms that the higher intensity light-granules stem from plasmonic hot spots and are not simply QD aggregates. Most of the high intensity occurrences exhibit a clear linear polarization dependance. Fig.3**(b)** shows the photoluminescence of the same sample area whilst exciting with a linearly polarized light. Pixels with an intensity below 83 % of the maximum pixel intensity were set to zero in order to highlight only

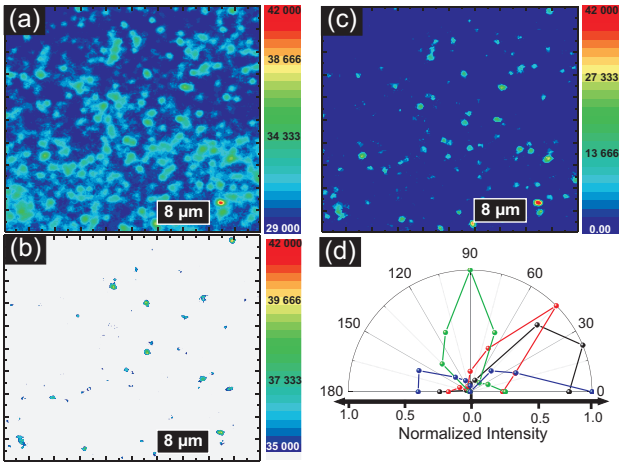

FIG. 3: False color plot of the colloidal quantum dot photoluminescence on a silver nano-island film: (a) Un-polarized, (b) linearly polarized, and (c) sum of all the linearly polarized luminescence images. (d) Normalized intensity of individual high-intensity photoluminescence hot spots as a function of the excitation linear polarization angle.

the high intensity events. We apply this same numerical *flooding* process[19] for a range of linear polarizations from 0^o to 180^o in steps of 22.5^o. The multiplication of all these images yields a featureless image, proving that all of the high intensity center emitted by the QDs on the silver film are linearly polarized. Figure 3**(c)** shows the sum of all the polarization dependent images divided by the number of images. This procedure allows us to clearly identify the position of the hot spots and evaluate their polarization dependance individually. The hot spot density is $(0.050\pm0.002)\,\mu\mathrm{m}^{-2}$. Each hot spot reaches a maximum value at a different polarization angle. The normalized hot spot intensity as a function of the polarization angle is presented in figure 3**(d)** for four different, but typical, hot spots. The hot spot intensity has been normalized with respect to its maximum (I_{max}) and minimum intensity (I_{min}).

The average of all of the polarization-dependent maximum pixel values is 130 000 counts/(J/cm^2). On the other hand, the average hot spot normalized pixel intensity for the silver films without any QDs is 3 900 counts/(J/cm^2). Thus, the average hot spot-induced QD photoluminescence enhancement is 190× the average value for QDs on bare quartz. The best pixel in the best hot spot yields a luminescence enhancement factor of 240×. These values are strikingly higher than those reported for lithography-defined films in Ref.[4].

We believe the linearly polarized hot spots originate from small gaps (few nanometers) between two or more adjacent silver nano-islands. An example of such a situation is shown on Fig.1**(b)**. It has been shown that such plasmonic dimers can generate very strong local field enhancements where the emitter quantum efficiency is greatly increased due to the Purcell effect[2, 17, 18]. Moreover, it was shown in Ref.[18] that arrays of metallic nano-particles can generate even higher spontaneous emission rate enhancements. Whilst the average distance between neighboring nano-islands is ≈16 nm, it is clear from the random film formation process that smaller distances occur in our experiment. This expectation is confirmed by the AFM measurement presented in Fig.1**(a)**. Moreover, the highest local field enhancement is not produced for the smallest inter-island spacing, but for an optimal value that depends on the wavelength, and dielectric constant of the metal and surrounding material [2, 17] . The low density of hot spots $(0.050\pm0.002)\,\mu\mathrm{m}^{-2}$ compared to the density of silver nano-islands $(230\pm10)\,\mu\mathrm{m}^{-2}$ is in good agreement with the nano-island formation process and the resulting Gaussian distribution of the nano-island sizes and positions.

In conclusion, we produced high quality silver-based plasmonic films with smooth half-spheroidal nano-islands. With a 10 nm-thick SiO_2 spacer, the photoluminescence of a layer of CdSe/ZnS colloidal QDs is enhanced on average by a factor of 160 compared to a nominally equal layer on bare quartz. We also observed the formation of polarization-dependent hot spots where the photoluminescence is on average enhanced by a factor of 190 and maximally by a factor of 240. The hot spots are believed to occur in gaps between nano-islands where two or more islands are coupled to generate very large electric fields.

This project was supported by the Deutsche Forschungs Gemeinschaft via the Nanosystems Initiative Munich. SF acknowledges support from the Alexander von Humboldt Foundation.

[1] V. Ferry, et al., Appl. Phys. Lett. **95**, 183503 (2009).
[2] H. Shen, et al., J. Appl. Phys. **106**, 073109 (2009).
[3] J. Hugall, et al., Appl. Phys. Lett. **95**, 141111 (2009).
[4] P. Pompa, et al., Nature Nano. **1**, 126 (2006).
[5] T. Ozel, et al., New J. Phys. **10**, 083035 (2008).
[6] I. Soganci, et al., Opt. Express **15**, 14289 (2007).
[7] R. Banerjee, et al., Phys. Rev. E **80**, 056204 (2009).
[8] K. Aslan, et al., J. Appl. Phys. **103**, 084307 (2008).
[9] F. Beck, et al., J. Appl. Phys. **105**, 114310 (2009).
[10] V. Komarala, et al., Appl. Phys. Lett. **93**, 123102 (2008).
[11] N. Borys, et al., Phys. Rev. B **80**, 161407(R) (2009).
[12] Y. Fu, et al., Chem. Phys. Lett. **447**, 96 (2007).
[13] J. Lakowicz, et al., Analyst **133**, 1308 (2008).
[14] V. Komarala, et al., Appl. Phys. Lett. **89**, 253118 (2006).
[15] K. Catchpole and A. Polman, Appl. Phys. Lett. **93**, 191113 (2008).
[16] L. Peyser, et al., Science **291**, 103 (2001).
[17] M. Ringler, et al., Phys. Rev. Lett. **100**, 203002 (2008).
[18] O. Muskens, et al., Nanoletters **7**, 2871 (2007).
[19] This numerical procedure sets all pixels with an intensity inferior to the specified threshold to zero.